# Geometric Numerical Integration of Simple Dynamical Systems

Patrick R. Schmitt and Paul Steinmann
University of Kaiserslautern
Chair of Applied Mechanics
Department of Mechanical and Process Engineering
D-67653 Kaiserslautern, Germany
prschmit@rhrk.uni-kl.de

**Abstract:** Understanding the behavior of a dynamical system is usually accomplished by visualization of its phase space portraits. Finite element simulations of dynamical systems yield a very high dimensionality of phase space, i.e. twice the number of nodal degrees of freedom. Therefore insight into phase space structure can only be gained by reduction of the model's dimensionality. The phase space of Hamiltonian systems is of particular interest because of its inherent geometric features namely being the co-tangent bundle of the configuration space of the problem and therefore having a natural symplectic structure. In this contribution a class of geometry preserving integrators based on Lie-groups and -algebras is presented which preserve these geometric features exactly. Examples of calculations for a simple dynamical system are detailed.

## 1 Introduction

In order to study the behaviour of dynamical systems one usually makes use of the theory of Hamiltonian systems and the phase-space concept. Within Hamilton's framework a dynamical system with $n$ degrees of freedom (DOFs) is described by generalized coordinates $q_k \in \mathbb{R}$ and corresponding canonical momenta $p_k \in \mathbb{R}$ for $k = 1, \dots, n$. The scalar Hamiltonian $H : \mathbb{R}^n \times \mathbb{R}^n \times \mathbb{R} \to \mathbb{R}$ is sufficient to describe the dynamics of the system completely. The equations of motion are Hamilton's equations:

$$\dot{p}_k = -\frac{\partial H(q,p,t)}{\partial q_k}, \qquad \dot{q}_k = \frac{\partial H(q,p,t)}{\partial p_k}, \quad k = 1, \dots, n$$

Solutions to this system of $2n$ ordinary differential equations are curves $(q(t), p(t)) \in \mathbb{R}^{2n}$ in *phase-space*.

To illustrate the phase-space concept figure 1 depicts one of the most simple dynamical systems, i.e. the 2-dimensional mathematical pendulum. Solution curves are clearly divided by a separatrix into two regions of vastly different behaviour. In the neighorhood of the origin of the coordinate system the pendulum is in normal back-and-forth oscillatory

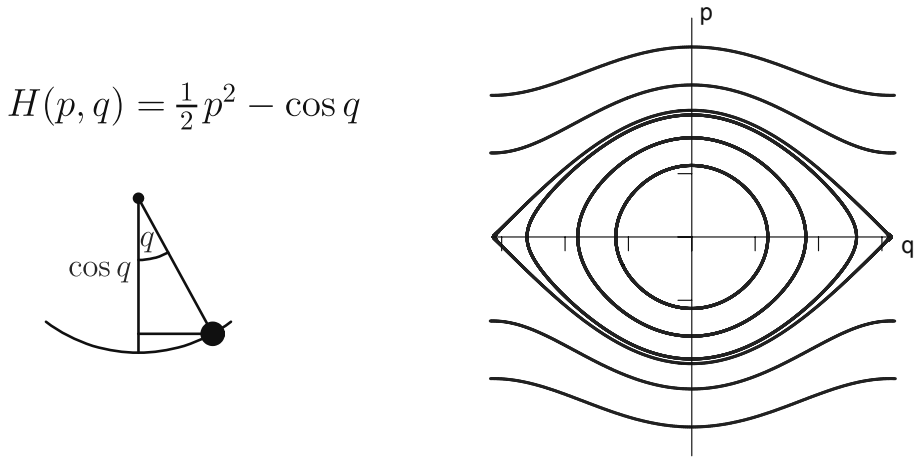


Figure 1: 2-dimensional mathematical pendulum in "natural" units, gravity acting downwards (left) and its phase-space portrait (right)

motion (closed, ellipsoidal solution curves). The outer region describes clockwise and counterclockwise spinning motion.

The dynamics of engineering structures are usually modelled by finite element simulations which leads to high dimensionality of phase spaces, i.e. twice the number of nodal degrees of freedom. Even small academic examples like the rotor blade shown in the upper left quadrant of figure 2 have a huge number of DOFs, in this case 716. The time-evolution of this freely flying rotor blade was determined by solving Hamilton's equations with an enhanced Galerkin method [Gro04]. The three quadrants labeled "phase-space projection" show different views of the $\{q_1, p_1, p_2\}$-projection for an arbitrarily chosen node. Obviously projection to an only 3-dimensional subspace of a vastly higher dimensional phase-space can not yield insight into the overall phase space structure.

Inspired by ideas from [MR94, SK03] we therefore turn to a geometrized version of Hamiltonian dynamics. The (finite dimensional) configuration space of a physical system has the structure of a (smooth) manifold and is denoted by $Q$. The momentum phase-space of this system is just the cotangent bundle $T^*Q$ which is equipped with a natural symplectic structure $\omega$ (a 2-form in the language of differential geometry). The Hamiltonian is a smooth map $H : T^*Q \to \mathbb{R}$ and the corresponding Hamiltonian vector field is denoted $X_H$ and determined by $dH = \omega(X_H, .)$. Hamilton's equations are just the equations of the flow of the vector-field $X_H$.

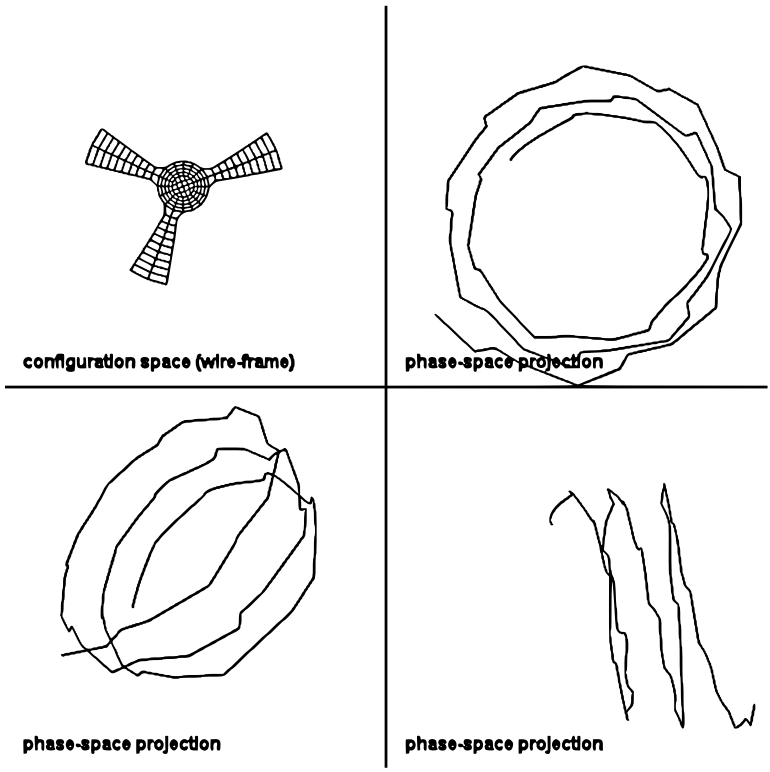


Figure 2: freely flying 2-dimensional hyper-elastic rotor blade, 140 4-node elements $\rightarrow$ 716 DOFs, different views of the $\{q_1, p_1, p_2\}$-projection for a single node

## 2 Geometric integration (Lie-group methods)

In order to exploit the geometric sructure of Hamiltonian dynamics to the fullest extent, we have to consider integration schemes that generate solutions which remain in the cotangent bundle of the configuration manifold $T^*Q$. In recent years a powerful machinery of geometric integration (especially Lie-group integrators) has been developed, see for example [FMMK99, IMNZ00, HLW02]. We will present its basic ingredients in the following subsections.

### 2.1 Lie-groups and Lie-algebras

We will start by looking at Lie-groups. A Lie-group is a group with a smooth (differentiable) group operation and smooth inversion. Therefore it can also be viewed as a

differentiable manifold. Several well-known examples [Olv93] are listed below:

$$\begin{aligned} GL(n,\mathbb{R}) &= \{g \in Mat(n\times n,\mathbb{R}) | \det g \neq 0\} && (1)\\ SL(n,\mathbb{R}) &= \{g \in GL(n,\mathbb{R}) | \det g = 1\} && (2)\\ O(n,\mathbb{R}) &= \left\{g \in GL(n,\mathbb{R}) | g^T g = e\right\} && (3)\\ SO(n,\mathbb{R}) &= \{g \in O(n,\mathbb{R}) | \det g = 1\} && (4) \end{aligned}$$

The Lie-algebra $\mathfrak{g}$ corresponding to a Lie-group $G$ can be defined as the tangent space to the group at the identity element $e \in G$

$$\mathfrak{g} = T_e G.$$

$\mathfrak{g}$ is a vector space equipped with a skew-symmetric, bilinear product called Lie-bracket

$$[\,.\,,\,.\,] : \mathfrak{g}\times\mathfrak{g} \to \mathfrak{g}$$

which satisfies Jacobi's identity: let $a, b, c \in \mathfrak{g}$

$$[a,[b,c]] + [b,[c,a]] + [c,[a,b]] = 0.$$

The Lie-algebras corresponding to the Lie-groups (1)−(4) defined above are the following:

$$\begin{aligned} \mathfrak{gl}(n,\mathbb{R}) &= \{X, Y \in Mat(n\times n,\mathbb{R}) | [X,Y] = XY - YX\} && (5)\\ \mathfrak{sl}(n,\mathbb{R}) &= \{X \in \mathfrak{gl}(n,\mathbb{R}) | \mathrm{tr} X = 0\} && (6)\\ \mathfrak{o}(n,\mathbb{R}) &= \left\{X \in \mathfrak{gl}(n,\mathbb{R}) | X^T + X = 0\right\} && (7)\\ \mathfrak{so}(n,\mathbb{R}) &= \mathfrak{o}(n,\mathbb{R}) && (8) \end{aligned}$$

Because of this tangent space construction there are several choices of coordinate charts that map from the Lie-algebra back to the Lie-group. One such coordinate chart is the exponential map $\exp : \mathfrak{g} \to G$ which maps the whole Lie-algebra to a neighbourhood of $e \in G$. Because of the smooth group operation required above, this map can be extended to the whole group $G$ via left- or right-translation. For matrix groups the exponential map is just the standard matrix exponential.

### 2.2 Lie-group and Lie-algebra actions

Lie-group and Lie-algebra actions describe the effect of group and algebra elements on points of a manifold, think of rotations $R \in SO(3)$ acting on points of $\mathbb{R}^3$ for example.
A (left) *Lie-group action* is a map

$$\Lambda : G \times \mathcal{M} \to \mathcal{M}.$$

It induces a corresponding *Lie-algebra action*

$$\lambda : \mathfrak{g} \times \mathcal{M} \to \mathcal{M}$$

via

$$\lambda(v,p) = \Lambda(\exp(v),p) \qquad v \in \mathfrak{g},\ p \in \mathcal{M}.$$

Next we define a map $\lambda_* : \mathfrak{g} \to \mathcal{X}(\mathcal{M})$ from the Lie-algebra to the set of vector-fields on $\mathcal{M}$ pointwise as

$$(\lambda_* v)(p) = \left.\frac{d}{dt}\right|_{t=0} \lambda(tv,p)$$

A differential equation on the manifold can now be written as

$$y' = \mathcal{F}_\lambda(t,y) = \left(\lambda_* f(t,y)\right)(y), \qquad y(0) = p \in \mathcal{M} \tag{9}$$

where $f : \mathbb{R} \times \mathcal{M} \to \mathfrak{g}$.

These definitions allow us to state the main paradigm of Lie-group methods as follows: The solution of the differential equation (9) for small $t \in \mathbb{R}^+$ is

$$y(t) = \lambda(u(t),p)$$

where $u(t) \in \mathfrak{g}$ satisfies

$$u' = \tilde{f}(u) = d\exp_u^{-1}\left(f(t,\lambda(u,p))\right), \qquad u(0) = 0 \in \mathfrak{g}. \tag{10}$$

This statement follows by the commutativity of the following diagram

$$\begin{array}{ccc} T\mathfrak{g} & \xrightarrow{\lambda'_p} & T\mathcal{M} \\ {\scriptstyle \tilde{f}}\uparrow & & \uparrow{\scriptstyle \mathcal{F}} \\ \mathfrak{g} & \xrightarrow[\lambda_p]{} & \mathcal{M} \end{array}$$

One problem we have not yet considered is the non-commutativity of general Lie-groups and Lie-algebras. Let $u_1, u_2 \in \mathfrak{g}$, then

$$\begin{array}{rrcl} \Lambda(\exp(u_1),\Lambda(\exp(u_2),p)) & = & \Lambda(\exp(u_1)\cdot\exp(u_2),p) \\ & = & \Lambda(\exp(\mathcal{B}(u_1,u_2),p) \\ \Rightarrow \qquad \lambda(u_1,\lambda(u_2,p)) & = & \lambda(\mathcal{B}(u_1,u_2),p) \end{array}$$

The symbol $\mathcal{B}(.,.)$ is the Baker-Campbell-Hausdorff formula which has the following explicit form in terms of iterated commutators

$$\begin{aligned} \mathcal{B}(u_1,u_2) \quad = \quad & u_1 + u_2 + \frac{1}{2}[u_1,u_2] \\ & + \frac{1}{12}[u_1,[u_1,u_2]] - \frac{1}{12}[u_2,[u_1,u_2]] + \ldots . \end{aligned}$$

In order to solve differential equations on manifolds it is sufficient to solve corresponding equations in the Lie-algebra which is a linear space. Therefore standard integration

schemes can be applied on the algebra-level and the solution mapped back to the nonlinear manifold via appropriate coordinate mappings. Suitable combinations of these have been developed in recent years, foremost the *Runge-Kutta-Munthe-Kaas* methods which usually require many iterated commutator evaluations and *Crouch-Grossman* methods which evaluate vector field flows via matrix exponentials.

## 3 A model system on the sphere $S^2$

This section sets out to illustrate the benefit of the presented geometric integration techniques. We introduce the following ordinary first-order differential equation on $\mathbb{R}^3$

$$\dot{\boldsymbol{x}} = \begin{bmatrix} -y + xz^2 \\ x + yz^2 \\ -z(x^2+y^2) \end{bmatrix}, \quad \boldsymbol{x} = \begin{bmatrix} x \\ y \\ z \end{bmatrix} \in \mathbb{R}^3. \tag{11}$$

A number of analytical observations on the behaviour of solutions to this equation can be made. Calculating the time derivative of the squared solution-norm yields

$$\begin{aligned} \frac{d}{dt}||\boldsymbol{x}(t)||^2 &= \frac{d}{dt}\left[\boldsymbol{x}(t)\cdot\boldsymbol{x}(t)\right] = 2\boldsymbol{x}(t)\cdot\dot{\boldsymbol{x}}(t) \\ &= 2\left[-xy + x^2z^2 + yx + y^2z^2 - z^2x^2 - z^2y^2\right] = 0 \end{aligned}$$

From this it is obvious that equation $(11)$ has spherical symmetry and it suffices to study its behaviour on the unit sphere $S^2 \subset \mathbb{R}^3$. Furthermore the problem restricted to $S^2$ has two fixed points (the poles $\boldsymbol{x}_\pm = [0,0,\pm 1]^T$) and an attractor (the equator $z(t) = 0\,\forall t$).

In order to use the Lie-group based methods introduced before we have to realize that $S^2$ can also be interpreted as a Lie-group, namely $S^2 \cong SO(3)$.
The corresponding Lie-algebra $T_eSO(3) = \mathfrak{so}(3)$ is the set of all skew-symmetric matrices and the exponential map $\exp : \mathfrak{so}(3) \to SO(3)$ is the standard matrix exponential.
In order to formulate equation $(11)$ on the Lie-algebra $\mathfrak{so}(3)$ we need another convenient fact namely $\mathfrak{so}(3) \cong \mathbb{R}^3$ via the hat-map

$$\mathbb{R}^3 \ni \boldsymbol{\omega} \mapsto \hat{\omega} = \begin{bmatrix} 0 & -\omega_3 & \omega_2 \\ \omega_3 & 0 & -\omega_1 \\ -\omega_2 & \omega_1 & 0 \end{bmatrix} \in \mathfrak{so}(3) \tag{12}$$

Since any vector-field on $S^2$ can be written as cross product $\boldsymbol{\omega} \times \boldsymbol{x}$ we get the differential equation on the algebra as

$$\dot{\boldsymbol{x}} = \begin{bmatrix} -y + xz^2 \\ x + yz^2 \\ -z(x^2+y^2) \end{bmatrix} = \begin{bmatrix} \omega_2 z - \omega_3 y \\ \omega_3 x - \omega_1 z \\ \omega_1 y - \omega_2 x \end{bmatrix} = \boldsymbol{\omega} \times \boldsymbol{x}$$

where obviously $\boldsymbol{\omega} = \left[-z[x+y], z[x-y], x^2+y^2\right]^T$. Therefore using the definition of

the hat-map $(12)$ a Lie-type integrator with fixed stepsize $h$ takes the following form

$$\boldsymbol{x}_{n+1} = \exp\left(h\hat{\omega}_n\right)\boldsymbol{x}_n = \exp\left(h\begin{bmatrix} 0 & -[x_n^2+y_n^2] & z_n[x_n-y_n] \\ x_n^2+y_n^2 & 0 & z_n[x_n+y_n] \\ -z_n[x_n-y_n] & -z_n[x_n+y_n] & 0 \end{bmatrix}\right)\boldsymbol{x}_n.$$

We compare this geometric integrator with three classic integration schemes that do not take into account the symmetry of the problem: Euler-forward, Euler-backward (both with fixed step-size) and a standard 4th order Runge-Kutte scheme with variable step-size (MATLAB ode45).

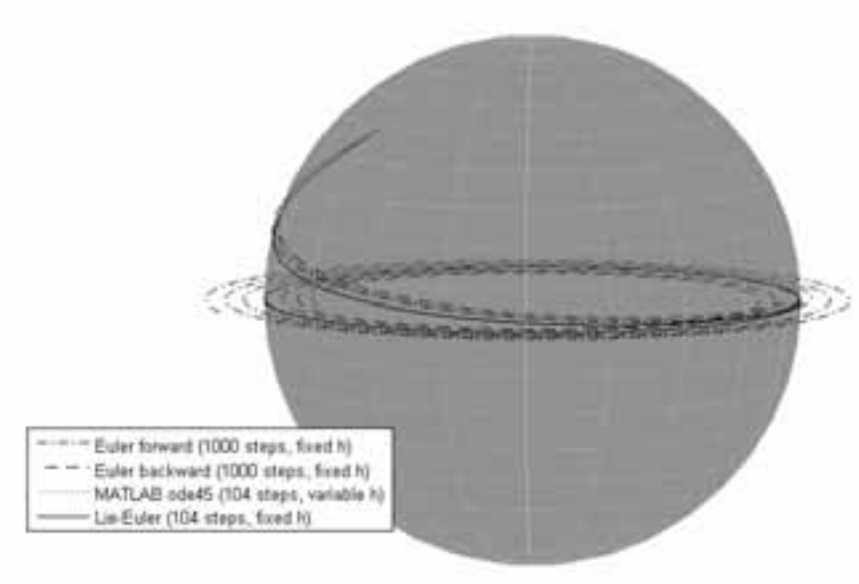


Figure 3: Solution trajectories "on" $S^2$ for the start value $\left[\frac{1}{\sqrt{3}}, \frac{1}{\sqrt{3}}, \frac{1}{\sqrt{3}}\right]^T$. Note that the Euler-forward and Euler-backward solutions both drift away from the solution manifold (outwards and inwards respectively) while the standard 4th order Runge-Kutta (MATLAB ode45) and the Lie-Euler scheme seem to perform much better even with only approximately 10% of the number of steps.

We start the computation at an initial value $\boldsymbol{x}(0) = \left[\frac{1}{\sqrt{3}}, \frac{1}{\sqrt{3}}, \frac{1}{\sqrt{3}}\right]^T$ and choose stepsizes for the classic Euler-forward and Euler-backward schemes as $0.02$, $0.04$, $0.002$ and $0.0002$ while fixing the number of steps for MATLAB ode45 and the geometric Lie-Euler-scheme at 104. The rather poor performance of the standard Euler-schemes with regard to preserving the spherical symmetry of equation $(11)$ is apparent in figure 3.

Because the 3-dimensional plot employed before is insufficient to determine the amount of deviation from the exact solution manifold we calculate the vector-norm for the different solution schemes and plot them in figure $4$ for the standard Euler stepsize of $0.002$. While

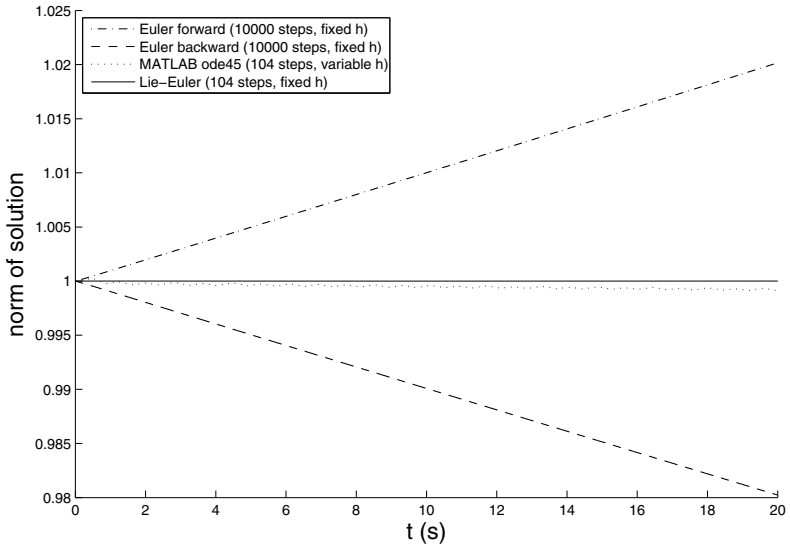


Figure 4: Deviation of trajectories from the configuration manifold $S^2$ for the different integration schemes illustrated by the fact that $\boldsymbol{x}(t) \in S^2 \Leftrightarrow ||\boldsymbol{x}(t)|| = 1$.

the classic Euler-schemes still deviate strongly from the expected result of $||\boldsymbol{x}(t)|| = 1$ for this step-size, both the standard 4th order Runge-Kutta and the Lie-Euler scheme perform rather well with only 104 steps.

Since the equator is an attractor of the differential equation an exact analytical solution can be stated for start values $z(0) = 0$ as

$$\boldsymbol{x}(t) = \begin{bmatrix} \cos(\varphi_0 + t) \\ \sin(\varphi_0 + t) \\ 0 \end{bmatrix} \qquad \varphi_0 \in \mathbb{R}.$$

Using this result the deviation of the four numerical integration schemes from the exact solution on the equator can be investigated. A start value $\varphi_0 = 0.5\,\pi$ is choosen and the stepsize for the standard Euler-schemes is varied in the same manner as above.

Figure 5 illustrates the fact that in order to reach an approximately equivalent accuracy the number of steps for the two standard Euler-schemes has to be increased to about 1000 times the number of MATLAB ode45 steps. Also note that the Lie-Euler integrator produces the exact solution up to machine precision with only 104 steps.

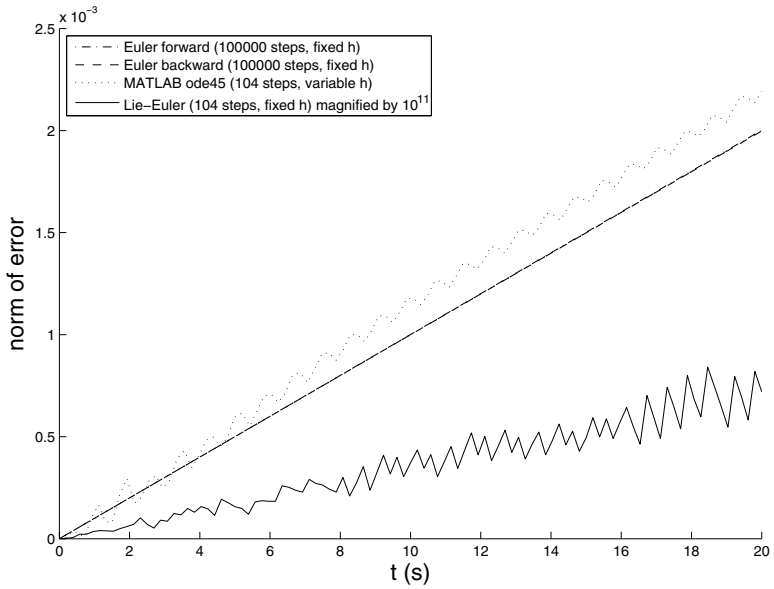


Figure 5: Comparison to the exact analytical solution on the equator of $S^2$. Note that the error of the Lie-Euler integrator is scaled by a factor of $10^{11}$. The error values of the two classic Euler schemes are almost indistinguishable.

# 4 Conclusions

In this contribution we have demonstrated the common problems in understanding the dynamic behaviour of engineering structures caused by the high dimensionality of their respective phase-spaces. In order to reduce this high dimensionality simpler model systems had to be studied. The intrinsic geometric structure of the Hamiltonian framework of dynamics led to the consideration of geometry preserving integrators of Lie-type. An example system has been cast into this Lie-type framework which made its dynamics approachable by new geometric numerical integration schemes. A comparison with standard integration schemes showed the superiority of this specific geometric integration scheme.

**Acknowledgements** Financial support by the DFG within the IRTG 1131 is gratefully acknowledged.

## References


[FMMK99] Stig Faltinsen, Arne Marthinsen, and Hans Z. Munthe-Kaas. Multistep Methods Integrating Ordinary Differential Equations on Manifolds. Technical Report Numerics No. 3/1999, The Norwegian University of Science and Technology, Trondheim, Norway, 1999.

[Gro04] M. Groß. *Conserving Time Integrators for Nonlinear Elastodynamics*. Dissertation, Lehrstuhl für Technische Mechanik, Technische Universität Kaiserlautern, 03 2004.

[HLW02] E. Hairer, C. Lubich, and G. Wanner. *Geometric Numerical Integration: Structure-Preserving Algorithms for Ordinary Differential Equations*, volume 31 of *Springer series in computational mathematics*. Springer-Verlag, New York, 2002.

[IMNZ00] A. Iserles, H. Z. Munthe-Kaas, S. P. Nørsett, and A. Zanna. Lie-group methods. *Acta Numerica*, 9:215–365, 2000.

[MR94] Jerrold E. Marsden and Tudor S. Ratiu. *Introduction to Mechanics and Symmetry*. Texts in appliexd mathematics. Springer Verlag, New York, 1994.

[Olv93] Peter J. Olver. *Applications of Lie Groups to Differential Equations*. Graduate Texts in Mathematics. Springer Verlag, New York, 2nd edition, 1993.

[SK03] J. J. Sławianowski and V. Kovalchuk. Invariant Geodetic Problems on the Affine Group and Related Hamiltonian Systems. *Rep. Math. Phys.*, 51(2/3):371–379, 2003.